

## The Thioacetate-Functionalized Self-Assembled Monolayers on Au: Toward High-Performance Ion-Selective Electrode for Ag<sup>+</sup>

Jian Jin, Wei-jie Zhou, Ying Chen, Yi-long Liu, Xiao-qiang Sun, and Hai-tao Xi\*

Key Laboratory of Fine Petrochemical Engineering, Changzhou university, Changzhou, Jiangsu 213164, P.R. China

\*E-mail: xihaitaocczu@gmail.com

Received August 5, 2013, Accepted December 3, 2013

Two classes of morpholino-substituted thioacetate have been successfully synthesized and their electrochemical properties of self-assembled monolayers (SAMs) on Au electrode are measured by cyclic voltammetry (CV) and electrochemical impedance spectroscopy (EIS). The barrier property of the SAMs-modified surfaces is evaluated by using potassium ferro/ferricyanide. The results suggest that the arenethioacetate forms higher-quality close-packed blocking monolayers in comparison with alkanethioacetate. Furthermore, it has shown that the barrier properties of these monolayers can be significantly improved by mixed SAMs formation with decanethiol. From our experimental results we find that the electron transfer reaction of [Fe(CN)<sub>6</sub>]<sup>3-/4-</sup> redox couple occurs predominantly through the pinholes and defects present in the SAM and both SAMs show a good and fast capacity in recognition for Ag<sup>+</sup>. The morphological and elementary composition have also been examined by scanning electron microscope (SEM) and energy dispersive spectrometer (EDS).

**Key Words :** SAMs, Cyclic voltammetry, Electrochemical impedance spectroscopy, Ion recognition

### Introduction

In recent years, self-assembled monolayers (SAMs) have provoked intense interest due to their nanometer size, highly-ordered structures and ion recognition properties.<sup>1,2</sup> Organosulfur compounds and their derivatives are particularly attractive due to their ease of preparation and the spontaneous adsorption and organization of them on the gold electrode surfaces to form the extraordinary ordered monolayers through self-assembling.<sup>3-6</sup> A number of applications for such SAMs have been explored, including nanolithography and chemical sensors.<sup>7-9</sup> Notably, SAMs have been employed in organic electronic devices to modify the work function of the electrodes.<sup>10-14</sup>

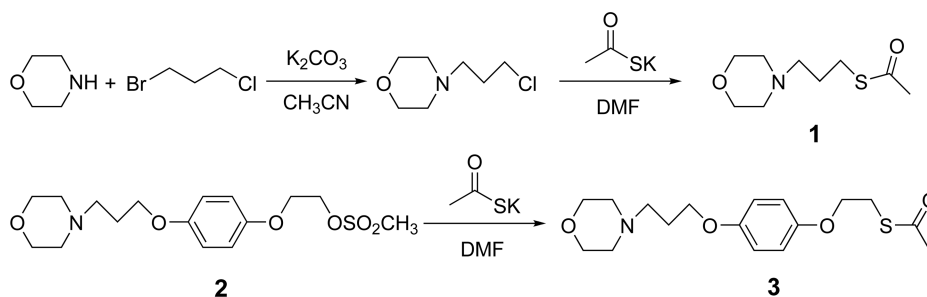
Self-assembled monolayers (SAMs) are formed at a solid-liquid interface by molecules consisted of three units: a headgroup that binds to the substrate, a tailgroup that constitutes the outer surface of the film, and a backbone, usually a long chain, that connects the headgroup and the tailgroup. While pure alkylthiols are known to form SAMs that exhibit order on a large scale,<sup>15-18</sup>  $\pi$ -conjugated thiols and their derivatives seem to be a better choice for applications in

organic- and single-molecule electronics because of their intrinsic semiconducting properties. Relatively recently, Piotrowski *et al.*<sup>19</sup> reported the synthesis and electronic properties of thioacetate-functionalized fullerene, Park *et al.*<sup>20</sup> studied the formation of octylthioacetates SAMs on gold in the vapor phase. Moreover the monolayer films based on aromatic sulfur compounds offer an opportunity to enhance the electrical coupling between the electronic states of the electrode and the redox species in solution.

Herein, we design two classes of morpholino-substituted thioacetate, and the different barrier property of the monolayer films formed on Au electrode is studied by using electrochemical techniques. The ion recognition properties of self-assembled monolayers using cyclic voltammetry are studied. We find that the arenethioacetate forms higher-quality close-packed organic layers than alkanethioacetate and both of them have an apparent and fast capacity in recognition for Ag<sup>+</sup>.

### Experimental

**Materials.** Synthesis and characterization of *S*-(3-morpho-



Scheme 1

linopropyl) ethanethioate (**1**), 2-(4-(3-morpholinopropoxy)phenoxy) ethyl methanesulfonate (**2**)<sup>21</sup> and *S*-(2-(4-(3-morpholinopropoxy)phenoxy)ethyl)ethanethioate (**3**) (Scheme 1) had been described elsewhere in detail.<sup>22</sup> All chemicals were analytical grade and used without further purification.

**Preparation of Substrates.** The gold disk electrode (CHI, 2 mm in diameter) was pretreated using the following procedure prior to monolayer deposition. The electrode was cleaned in piranha solution, which is a mixture of 30% H<sub>2</sub>O<sub>2</sub> and concentrated H<sub>2</sub>SO<sub>4</sub> in 1:3 ratios. Then it was polished with alumina powder (diameter, 0.3 and 0.05 μm) followed by sonication in ethanol and deionized water. After copious rinsing with deionized water, the electrode was electrochemically cleaned by cycling the potential from 0.5 to 1.6 V at 50 mV s<sup>-1</sup> in 0.5 M sulfuric acid until typical cyclic voltammogram of clean gold was obtained.<sup>23,24</sup>

**Preparation of SAMs and Mixed SAMs.** The pretreated gold electrodes were immersed in 10 mM **1** and **3** acetone solution for about 24 h at ambient temperature (25 ± 1 °C) respectively. Then the modified electrodes were removed from the solution and rinsed with deionized water, and dried with high purity nitrogen. The SAMs-modified gold electrodes were obtained and used for the electrochemical measurements immediately.

We had further tried to improve the blocking ability by forming a mixed SAMs with decanethiol. Immediately after the adsorption of corresponding compounds, the monolayer coated electrodes were rinsed with deionized water and dipped in 10 mM decanethiol-methanol solution for mixed SAMs formation. After 10 h at ambient temperature, the mixed SAMs modified electrodes were rinsed with deionized water and dried with high purity nitrogen, and subsequently analyzed using electrochemical studies.

**Electrochemical Measurements.** Electrochemical measurements were conducted by a PC controlled CHI920C electrochemical workstation bipotentiostat (CHI, Shanghai Chenhua Co.). A conventional three-electrode electrochemical cell with a Pt wire as a counter electrode, a Ag/AgCl (3 M KCl) electrode as a reference electrode and SAM-modified Au electrode as working electrode was used for the electrochemical characterization of SAMs.

Cyclic voltammetry (CV) measurements were operated in 5 mM K<sub>3</sub>[Fe(CN)<sub>6</sub>] with 0.1 M KCl at a potential range of -0.2 to 0.5 V. The impedance measurements were carried out using an ac signal of 10 mV amplitude at a formal potential of the redox couple at a wide frequency range of 100 kHz to 0.1 Hz. From the impedance data, the charge transfer resistance (R<sub>ct</sub>) was determined using the equivalent circuit fitting analysis. The impedance spectroscopy data were used for the equivalent circuit fitting analysis using ZSimpwin software.

## Results and Discussion

**Cyclic Voltammetry.** Figure 1 showed the cyclic voltammograms of bare Au and SAMs-modified electrodes in 5 mM [Fe(CN)<sub>6</sub>]<sup>3-/4-</sup> with 0.1 M KCl at a potential scan rate of 50

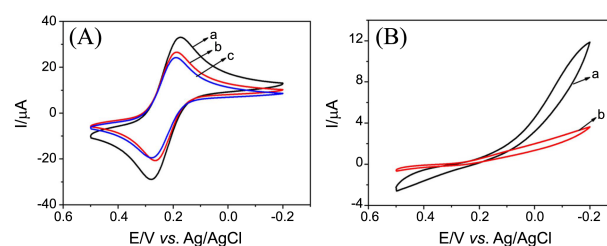


**Figure 1.** (A) Cyclic voltammograms of Au (a), **1**/Au (b), **3**/Au (c) in 5.0 mmol/L K<sub>3</sub>[Fe(CN)<sub>6</sub>]/0.1 mol/L KCl. (B) Cyclic voltammograms of **1**/C<sub>10</sub>SH/Au (a), **3**/C<sub>10</sub>SH/Au (b) in 5.0 mmol/L K<sub>3</sub>[Fe(CN)<sub>6</sub>]/0.1 mol/L KCl. Scan rate: 50 mV s<sup>-1</sup>.

mV s<sup>-1</sup>. As it could be seen from Figure 1A(a), for the bare Au electrode, the reversible characteristic peak for the redox couple was observed, indicating that the electron transfer reaction was completely diffusion controlled. However, for the **1**/Au and **3**/Au electrodes (Figure 1A(b, c)), it was clearly seen that a significantly blocking behavior could be found. For the **1**/C<sub>10</sub>SH/Au and **3**/C<sub>10</sub>SH/Au electrodes (Figure 1B), no typical peak of the redox couple was observed. This might be ascribed to the fact that compound **1** (or **3**) and C<sub>10</sub>SH anchored on the surface of Au electrode assembled a highly ordered, compact monolayer which completely inhibited the redox reaction. It could also be observed that in the case of compound **3** (Figure 1A(c), Figure 1B(b)), the CVs exhibited a rather better blocking behavior, which indicated the compound structure had an effect on the form of SAMs. The arenethioacetate SAMs was dominated by the π-π interactions between the benzene rings, while the alkanethioacetate SAMs was driven by the van der Waals interactions between the CH<sub>2</sub> groups. Therefore arenethioacetate could form high-quality close-packed organic layers and had a bigger barrier for charge-carrier injection at the electrode-liquid interface.

Figure 2 showed the cyclic voltammograms of SAMs-

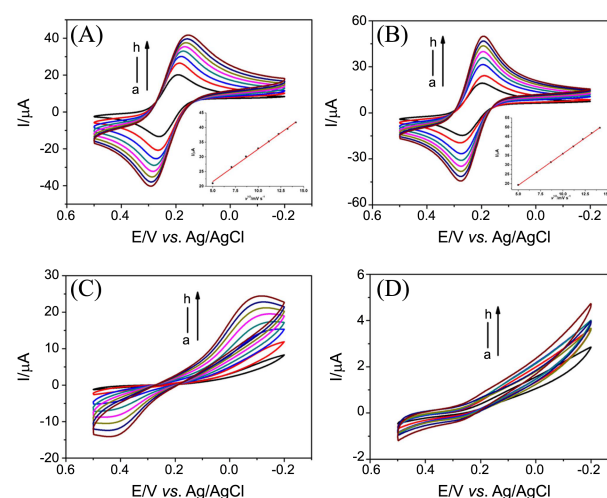


**Figure 2.** Cyclic voltammograms of **1**/Au (a), **3**/Au (b), **1**/C<sub>10</sub>SH/Au (c), **3**/C<sub>10</sub>SH/Au (d) in 5.0 mmol/L K<sub>3</sub>[Fe(CN)<sub>6</sub>]/0.1 mol/L KCl. Scan rate (from a to h): 25, 50, 75, 100, 125, 150, 175, 200 mV s<sup>-1</sup>. Inset: I<sub>pc</sub>-v<sup>1/2</sup>.

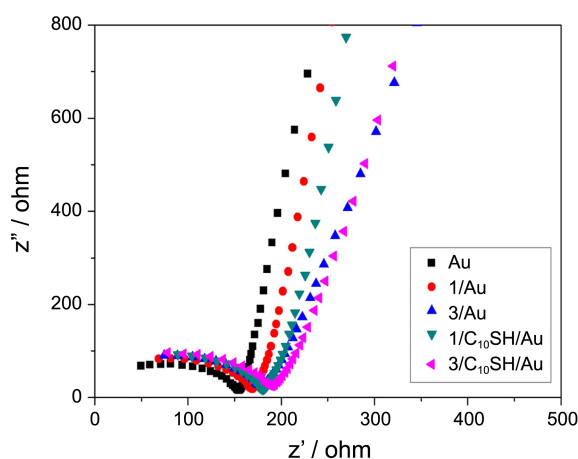


**Figure 3.** Impedance plots of Au, 1/Au, 3/Au, 1/C<sub>10</sub>SH/Au, 3/C<sub>10</sub>SH/Au in 5.0 mmol/L K<sub>3</sub>[Fe(CN)<sub>6</sub>]/0.1 mol/L KCl.

modified electrodes in 5 mM [Fe(CN)<sub>6</sub>]<sup>3-/4-</sup> at different scan rates. The corresponding insets of these Figures showed that the reductive peak current ( $I_{pc}$ ) had a direct linear relationship with the square root of scan rate. The linear regression equations were  $I_{pc} = 2.2205 v^{1/2} + 10.4728$  ( $R = 0.9974$ ),  $I_{pc} = 3.3552 v^{1/2} + 2.3873$  ( $R = 0.9999$ ), respectively, which meant the electron transfer process was essentially diffusion controlled.

**Electrochemical Impedance Spectroscopy.** Figure 3 showed the Nyquist plots of bare Au and SAMs-modified gold electrodes in 5 mM [Fe(CN)<sub>6</sub>]<sup>3-/4-</sup> with 0.1 M KCl. It could be seen from the Figure 3 that the bare Au electrode showed a low frequency straight line with a very small semicircle at high frequency region indicating that the electron transfer process was essentially diffusion-controlled. For the SAM or mixed SAMs modified electrodes, it could be seen that large semicircles at the high frequency region of impedance plots were observed, implying a good blocking behavior for the redox reaction. It could also be noted from Figure 3 that the impedance values were much higher in the case of SAM of compound 3, which indicated a better blocking ability of the SAM towards the redox reaction. The results were in conformity with our studies using cyclic voltammetry.

According to the data obtained from the Nyquist plots, the value of  $R_0$  and  $R_{ct}$  could be calculated (where  $R_0$  was the charge transfer resistance of bare Au electrode and  $R_{ct}$  was the charge transfer resistance of the corresponding different SAM-modified electrodes).  $R_{ct}$  was a measure of blocking ability of the monolayer films towards the electron transfer reaction. Higher the  $R_{ct}$  values better the blocking behaviour of monolayers. Table 1 showed some measured parameters of bare gold and SAM-modified electrodes obtained from the impedance plots. From the table the charge transfer resistance values, we could calculate the surface coverage ( $\theta$ ) of the monolayer on the gold electrode using equation  $\theta = 1 - (R_0/R_{ct})$ , by assuming that the current was attributed to the presence of pinholes and defects within the monolayer.<sup>25,26</sup> From the calculated  $R_{ct}$  and surface coverage

**Table 1.** The charge transfer resistance ( $R_{ct}$ ) and the surface coverage ( $\theta$ ) of compound 1 and 3 on the gold surface

Sample	Bare Au	1/Au	3/Au	1/C <sub>10</sub> SH/Au	3/C <sub>10</sub> SH/Au
$R_{ct}/\text{ohm}$	157.2	171.2	179.9	184.7	191.4
$\theta$	-	0.082	0.126	0.149	0.179

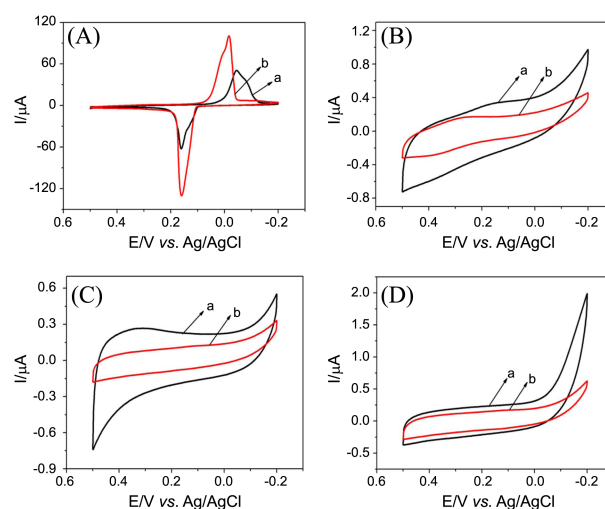


**Figure 4.** (A) Ag<sup>+</sup> at the SAMs of 1 (a), 3 (b) on Au electrode in 0.1 mol/L KCl; (B) Cu<sup>2+</sup> at the SAMs of 1 (a), 3 (b) on Au electrode in 0.1 mol/L KCl; (C) Pb<sup>2+</sup> at the SAMs of 1 (a), 3 (b) on Au electrode in 0.1 mol/L KCl; (D) Fe<sup>3+</sup> at the SAMs of 1 (a), 3 (b) on Au electrode in 0.1 mol/L KCl. Scan rate: 50 mV s<sup>-1</sup>.

values, it was clear that the blocking ability of these SAMs followed the order 3/Au > 1/Au.

**Ion Recognition.** Ag<sup>+</sup>, Cu<sup>2+</sup>, Pb<sup>2+</sup> and Fe<sup>3+</sup>, carrying different charges, were used to investigate the electrochemical properties of the 1/Au and 3/Au electrode. Immediately prior to use, the SAMs-modified Au electrodes were immersed in a freshly prepared 5 mM aqueous solution of silver nitrate,

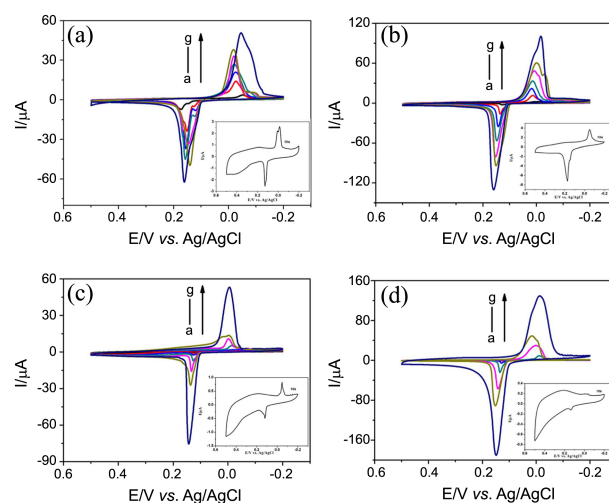


**Figure 5.** Cyclic voltammograms of 1/Au (A), 3/Au (B), 1/C<sub>10</sub>SH/Au (C), 3/C<sub>10</sub>SH/Au (D) electrode adsorbed Ag<sup>+</sup> in 0.1 mol/L KCl. Deposition time (from a to g): 10 s, 30 s, 60 s, 5 min, 30 min, 60 min, 4 h. Inset: deposition time at 10 s.

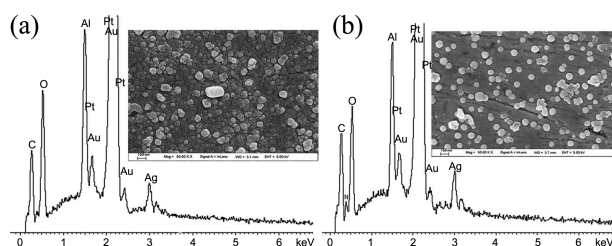


**Figure 6.** (a) SEM image and EDS spectrum of 1-silver modified electrode. (b) SEM image and EDS spectrum of 3-silver modified electrode.

copper sulfate, lead acetate and iron trichloride for 8 h followed by rinsing with deionized water. It could be seen from Figure 4(A) that the 1/Au and 3/Au electrode enriched of  $\text{Ag}^+$  showed reversible redox peaks indicating that  $\text{Ag}^+$  was adsorbed to the SAMs. In contrast, the absence of any peak formation in the CVs of  $\text{Cu}^{2+}$ ,  $\text{Pb}^{2+}$  and  $\text{Fe}^{3+}$  at the 1/Au and 3/Au electrodes (Figure 4(B), Figure 4(C), Figure 4(D)) indicated that they could not be adsorbed to the SAMs.

We had further studied the recognition speed of  $\text{Ag}^+$  on SAM-modified electrode. It could be seen from Figure 5 (inset), when the deposition time was 10 s, it showed a reversible redox peak. With the increase of deposition time, the current increased, which meant that more silver ions were adsorbed to the SAMs-modified electrode.

Furthermore, SEM, along with EDS measurements provide additional evidence about the recognition for  $\text{Ag}^+$ . Figure 6(a, b) showed the SEM and EDS analysis of SAMs of 1-silver and 3-silver. The Ag composition of them was 2.9% and 4.34% respectively.

## Conclusion

In this study, two different classes of thioacetate were synthesized: one class contained a alkyl chain, the other had a phenoxy backbone. Electrochemical techniques such as cyclic voltammetry and electrochemical impedance spectroscopy were employed to evaluate the barrier property of monolayer films using potassium ferro/ferri cyanide redox couple as a probe. We found from our results that the arene-thioacetate formed high-quality close-packed organic layers. The electron transfer reaction of  $[\text{Fe}(\text{CN})_6]^{3-/4-}$  was completely inhibited on the mixed SAMs modified surfaces. From the cyclic voltammograms of SAMs-modified electrodes, all of them had an apparent and fast capacity in recognition for  $\text{Ag}^+$ . SEM and EDS measurements had been used to prove it.

**Acknowledgments.** The authors are grateful for the financial support from the National Natural Science Foundation of China (No. 20872051). And the publication cost of this paper was supported by the Korean Chemical Society.

## References

1. Love, J. C.; Estroff, L. A.; Kriebel, J. K.; Nuzzo, R. G.; Whitesides,

- G. M. *Chem. Rev.* **2005**, *105*, 1103.
2. Zhang, S.; Cardona, C. M.; Echegoyen, L. *Chem. Commun.* **2006**, 4461.
3. Stouffer, J. M.; McCarthy, T. J. *Macromolecules* **1988**, *21*, 1204.
4. Burshtain, D.; Mandler, D. *J. Electroanal. Chem.* **2005**, *581*, 310.
5. Holmlin, R. E.; Chen, X. X.; Chapman, R. G.; Takayama, S.; Whitesides, G. M. *Langmuir* **2001**, *17*, 2841.
6. Li, Z. G.; Niu, T. X.; Zhang, Z. J.; Feng, G. Y.; Bi, S. P. *J. Analyst.* **2012**, *137*, 1680.
7. Eck, W.; Stadler, V.; Geyer, W.; Zharnikov, M.; Golzhauser, A.; Grunze, M. *Adv. Mater.* **2000**, *12*, 805.
8. Felgenhauer, T.; Yan, C.; Geyer, W.; Rong, H. T.; Golzhauser, A.; Buck, M. *Appl. Phys. Lett.* **2001**, *79*, 3323.
9. Hobara, D.; Imabayashi, S.; Kakiuchi, T. *Nano. Lett.* **2002**, *2*, 1021.
10. Zhang, Y.; Salaita, K.; Lim, J. H.; Mirkin, C. A. *Nano. Lett.* **2002**, *2*, 1389.
11. Zehner, R. W.; Parsons, B. F.; Hsung, R. P.; Sita, L. R. *Langmuir.* **1999**, *15*, 1121.
12. Alloway, D. M.; Hofmann, M.; Smith, D. L.; Gruhn, N. E.; Graham, A. L.; Colorado, R. J.; Wysocki, V. H.; Lee, T. R.; Lee, P. A.; Armstrong, N. R. *J. Phys. Chem. B* **2003**, *107*, 11690.
13. Campbell, I. H.; Rubin, S.; Zawodzinski, T. A. *J. P. Phys. Rev. B* **1996**, *54*, 14321.
14. Shon, Y. S.; Lee, T. R. *J. Phys. Chem. B* **2000**, *104*, 8192.
15. Yang, Y. T.; Jamison, A. C.; Barriet, D.; Lee, T. R.; Ruths, M. *J. Adhes. Sci. Technol.* **2010**, *24*, 2511.
16. Ma, F.; Lennox, R. B. *Langmuir* **2000**, *16*, 6188.
17. Yokota, Y.; Fukui, K. I.; Enoki, T.; Hara, M. *J. Phys. Chem. C* **2007**, *111*, 7561.
18. Lee, L. Y. S.; Lennox, R. B. *Langmuir* **2007**, *23*, 292.
19. Piotrowski, P.; Pawlowska, J.; Palys, B.; Sek, S.; Bilewicz, R.; Kaim, A. *J. Electrochem. Soc.* **2013**, *160*, H28.
20. Park, T.; Kang, H.; Kim, Y.; Lee, S.; Noh, J. *Bull. Korean Chem. Soc.* **2011**, *32*, 39.
21. Sun, Y. Q.; Xi, H. T.; Chen, Y.; Sun, X. Q.; Chin. *J. Syn. Chem.* **2013**, *21*, 200.
22. The synthesis and characterization of target compounds are summarized as follows: Compound **1**: 1-bromo-3-chloropropane (0.94 g, 6 mmol) was added to a solution of morpholine (0.26 g, 3 mmol) and  $\text{K}_2\text{CO}_3$  (0.83 g, 6 mmol) in  $\text{CH}_3\text{CN}$  (20 mL) and the resulting mixture was refluxed for 6 h. After cooling down, the filtrate was evaporated under vacuum to afford a yellow oil without further purification. Then it reacted with potassium thioacetate (0.69 g, 6 mmol) in DMF (20 mL) under stirring at R. T. for 3 h. Then the crude mixture was washed with  $\text{H}_2\text{O}$  and extracted with  $\text{CH}_2\text{Cl}_2$  for many times, dried ( $\text{Na}_2\text{SO}_4$ ), concentrated and purified through column chromatography (ethylacetate/petroleumether, 1:6) to get compound **1** (0.05 g, 10%).  $^1\text{H}$  NMR (300 MHz,  $\text{CDCl}_3$ )  $\delta$  3.71 (t,  $J = 4.4$  Hz, 4H), 2.92 (t,  $J = 7.2$  Hz, 2H), 2.43 (t,  $J = 4.5$  Hz, 4H), 2.40 (t,  $J = 7.3$  Hz, 2H), 2.33 (s, 3H), 1.79 (m, 2H).  $^{13}\text{C}$  NMR (75 MHz,  $\text{CDCl}_3$ )  $\delta$  195.8, 77.5, 76.7, 66.9, 57.5, 53.6, 30.6, 27.0, 26.5. Compound **3** (0.6 g, 90%) was obtained through the tran-esterification of compound **2** (0.72 g, 2 mmol) treated with potassium thioacetate (0.34 g, 3 mmol) under the similar process.  $^1\text{H}$  NMR (300 MHz,  $\text{CDCl}_3$ )  $\delta$  6.83 (s, 4H), 4.04 (t,  $J = 6.4$  Hz, 2H), 3.97 (t,  $J = 6.3$  Hz, 2H), 3.73 (t,  $J = 4.7$  Hz, 4H), 3.25 (t,  $J = 6.4$  Hz, 2H), 2.52 (t,  $J = 7.4$  Hz, 2H), 2.47 (t,  $J = 4.5$  Hz, 4H), 2.37 (s, 3H), 1.95 (m, 2H).  $^{13}\text{C}$  NMR (75 MHz,  $\text{CDCl}_3$ )  $\delta$  195.3, 153.5, 152.4, 115.6, 115.4, 77.6, 76.8, 67.2, 66.9, 66.6, 55.5, 53.7, 30.5, 28.5, 26.5.
23. Sanders, W.; Vargas, R.; Anderson, M. R. *Langmuir* **2008**, *24*, 6133.
24. Xi, H. T.; Ju, S. L.; Chen, Z. D.; Sun, X. Q. *Chem. Lett.* **2010**, *39*, 415.
25. Finklea, H. O.; Snider, D. A.; Fedyk, J.; Sabatani, E.; Gafni, Y.; Rubinstein, I. *Langmuir* **1993**, *9*, 3660.
26. Protsailo, L. V.; Fawcett, W. R. *Langmuir* **2002**, *18*, 8933.